

Supporting Information

Exceptional quenching properties of tetrazine-based organic frameworks for fluorescently labeled nucleic acids and their applications in sensing

Chenggang Liu,^{‡a} Yanfei Kang,^{‡b} Wenjiao Li^a, Cheng Yao^a and Chan Song*^a

^a School of Chemistry and Molecular Engineering, Nanjing Tech University, Nanjing 211816, China; Email: songchan@njtech.edu.cn

^b Tangshan Labor Technicians College, Tangshan, 063300, China

‡ These two authors contributed equally to this work.

Table S1. The oligonucleotides used in this work.

Oligonucleotides	Oligonucleotide Sequences
1-mer-FAM	5'-A-FAM-3'
2-mer-FAM	5'-CA-FAM-3'
3-mer-FAM	5'-CCA-FAM-3'
6-mer-FAM	5'-TAA CCA-FAM-3'
12-mer-FAM	5'-AGG CAG TAA CCA-FAM-3'
24-mer-FAM	5'-AGG CAG TAA CCA AGG CAG TAA CCA-FAM-3'
24-mer	5'-AGG CAG TAA CCA AGG CAG TAA CCA-3'
36-mer-FAM	5'-AGG CAG TAA CCA AGG CAG TAA CCA AGG CAG TAA CCA-FAM-3'
12-mer-Cy3	5'-AGG CAG TAA CCA-Cy3-3'
12-mer-ROX	5'-AGG CAG TAA CCA-ROX -3'
P-FAM	5'-FAM-AGT CAG TGT GGA AAA TCT CTA GC-3'
T	5'-GCT AGA GAT TTT CCA CAC TGA CTG AGA-3'
T1	5'-GCT AGA GAT TTC CCA CAC TGA CTG AGA-3'
T2	5'-GCT AGA GCT TTT CCA AAC TGA CTG AGA-3'
T3	5'-GCT TGA GAT ATT CCG CAC TCA CTG AGA-3'
T4	5'-CGA GGC GAT GCC GAA CTC GA-3'

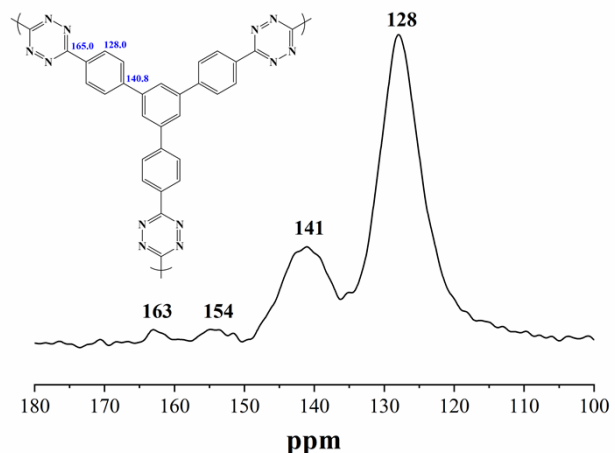


Figure S1. Solid ^{13}C NMR spectra of TzF-9.

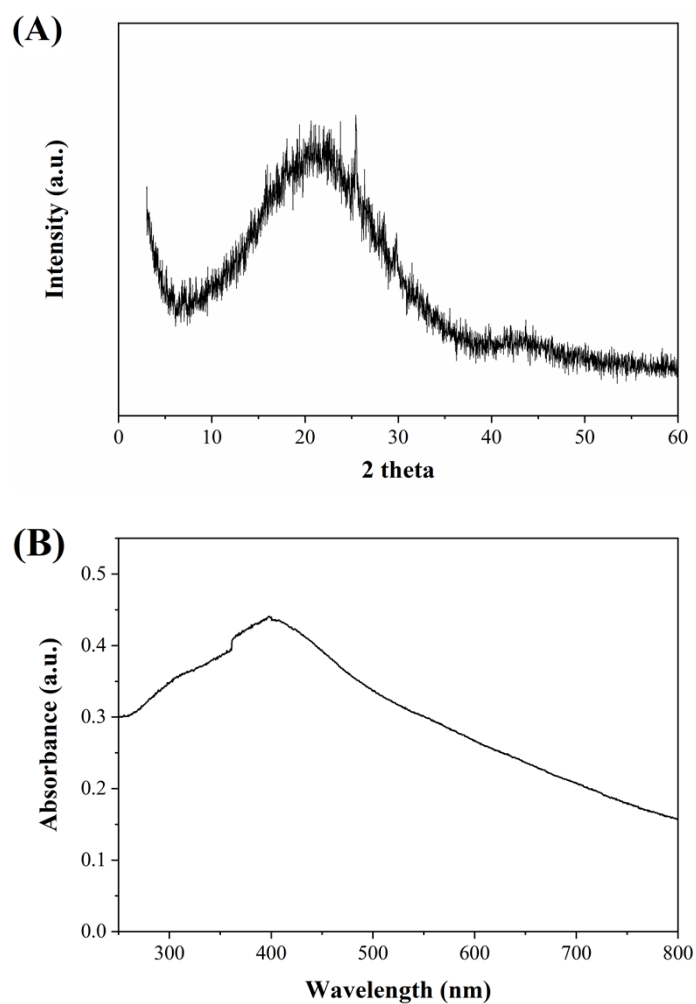


Figure S2. (A) X-ray powder diffraction patterns of TzF-9. (B) UV-vis spectrum of TzF-9 in water. $[\text{TzF-9}] = 20 \mu\text{g mL}^{-1}$.

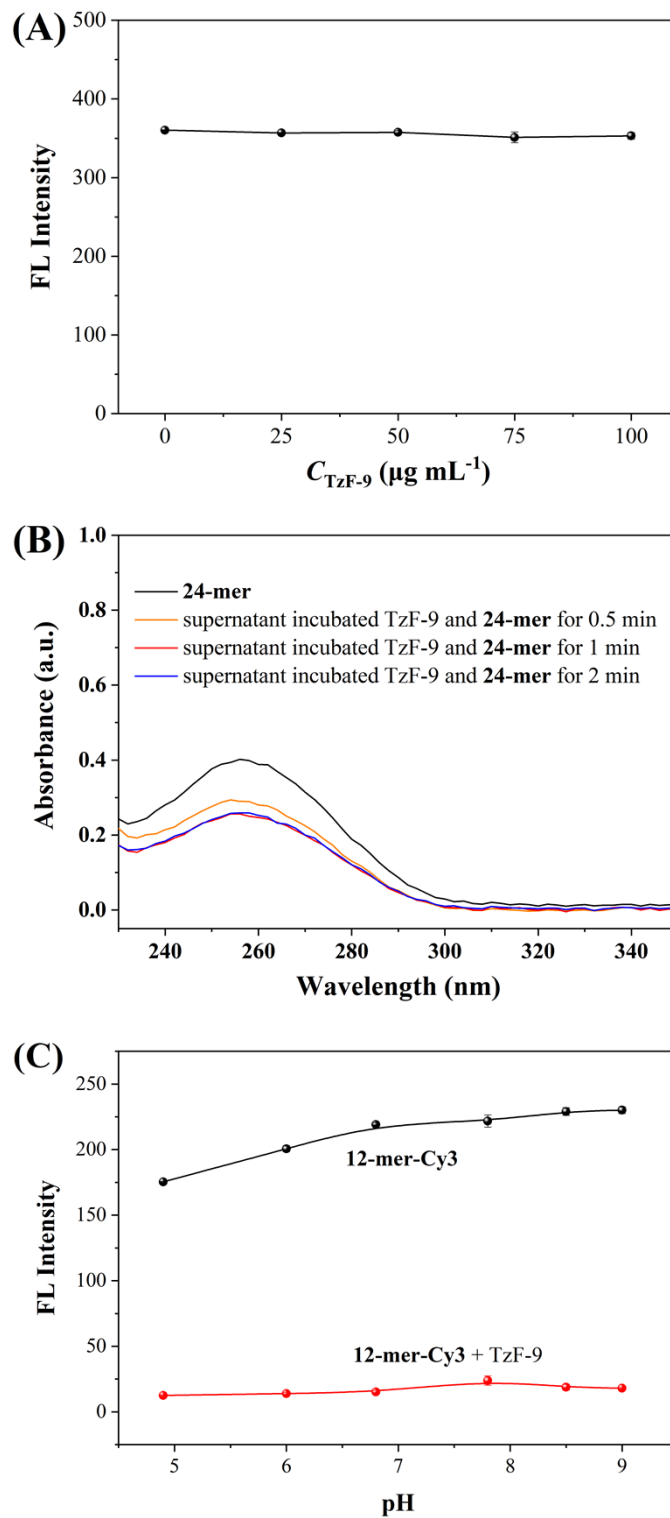


Figure S3. (A) Fluorescence intensity at 518 nm of fluorescein (free FAM) with the different amount of TzF-9. [free FAM] = 50 nM. (B) UV-vis spectra of **24-mer** and supernatant separated from the mixture that TzF-9 adsorbed **24-mer** with different incubating time. [**24-mer**] = 2 μM , [TzF-9] = 50 $\mu\text{g mL}^{-1}$. (C) Fluorescence intensities of **12-mer-Cy3** at 562 nm in the absence and presence of TzF-9 under different pH condition. [**12-mer-Cy3**] = 50 nM, [TzF-9] = 25 $\mu\text{g mL}^{-1}$.

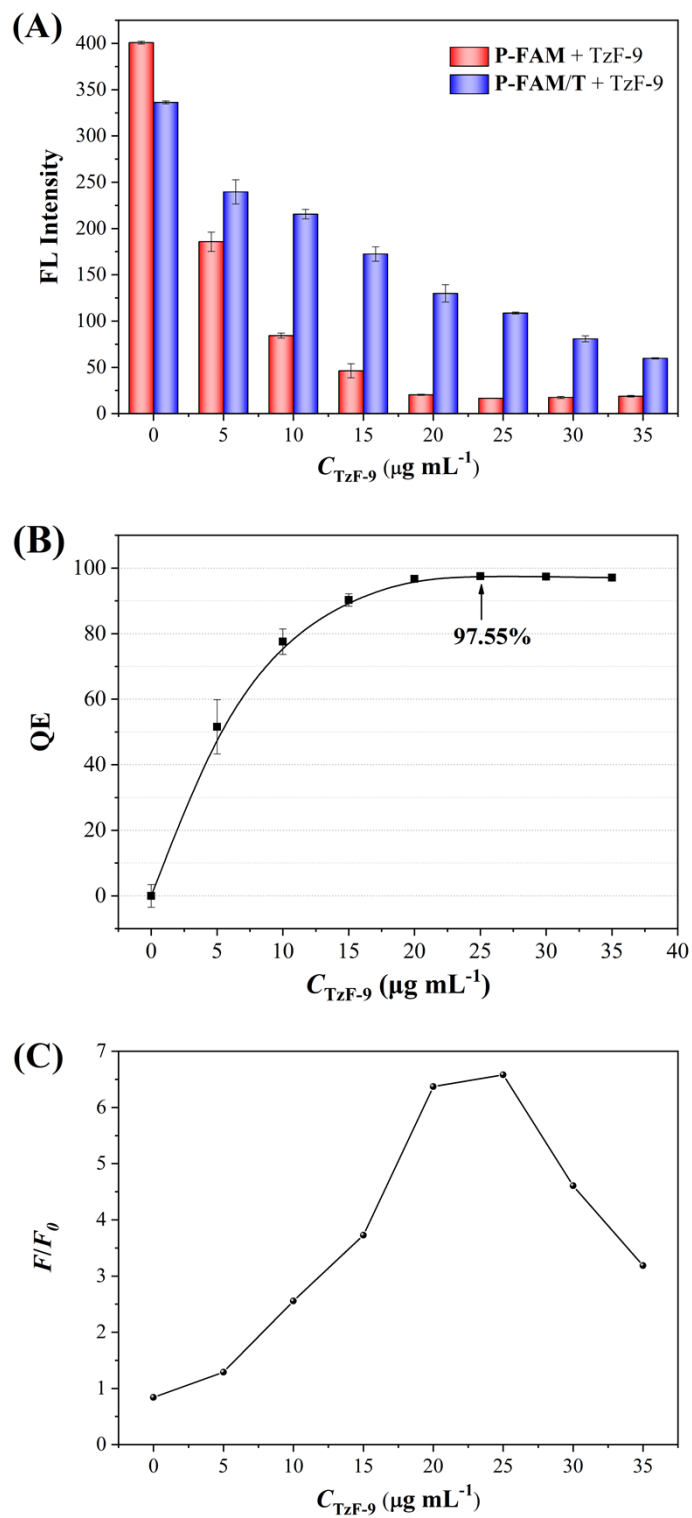


Figure S4. (A) Fluorescence intensity at 518 nm of **P-FAM** and **P-FAM/T** with different concentration of TzF-9. (B) Quenching efficiency of **P-FAM** induced by TzF-9. $[\text{P-FAM}] = 50 \text{ nM}$. (C) The signal-to-noise ratio (F/F_0) of sensing system with different concentration of TzF-9. F and F_0 are the fluorescence intensities at 518 nm of **P-FAM/T** and **P-FAM** with TzF-9, respectively. $[\text{P-FAM}] = 50 \text{ nM}$, $[\text{T}] = 50 \text{ nM}$.

Table S2. Comparison of different fluorescence quenchers as the sensing platform for assay of DNase I activity.

Quencher	Detection limit (U mL ⁻¹)	Linear range (U mL ⁻¹)	Reference
Ti ₃ C ₂ nanosheet	0.16	1-7	1
AuNPs	0.38	2-40	2
MG	1	5-100	3
GO	0.1	0-10	4
TzF-9	0.41	1-120	This work

Table S3. Analytical results for DNase I activities in 1% urine samples.

Sample	Added (U mL ⁻¹)	Determined (U mL ⁻¹)	Recovery (%)
1	0	—	—
2	10	10.2 ± 0.2	102.6 ± 2.0
3	100	101.5 ± 3.2	101.5 ± 3.2

Table S4. Comparison of different nanomaterial-based fluorescence quenchers as the sensing platforms for detection of ssDNA.

Quencher	Detection limit (nM)	Linear range (nM)	QE (%)	Reference
TNs	1.5	2-300	54	5
Pd NWs	6	10-100	88	6
SWCNH	1	1-100	83	7
MPC	1	3-150	90	8
PDA- <i>co</i> -SiO ₂ NPs	1	0-12	80	9
BQNPs	1.04	2-50	95	10
CuS NPs	0.8	0-20	95	11
TzF-9	0.79	1-125	95	This work

Table S5. Analytical results for ssDNA T in 1% urine samples.

Sample	Added (nM)	Determined (nM)	Recovery (%)
1	0	—	—
2	50	51.3 ± 1.8	102.6 ± 3.6
3	100	104.3 ± 0.9	104.3 ± 0.9

References

1. Peng, G.; Lin, B.; Guo, M.; Cao, Y.; Yu, Y.; Wang, Y., Enzyme activity termination by titanium carbide nanosheet and its application for the detection of deoxyribonuclease I. *Talanta* **2023**, *259*, 124533.
2. Liu, Y.; Xu, J.; Wang, Q.; Li, M.-J., Coupling coumarin to gold nanoparticles by DNA chains for sensitive detection of DNase I. *Anal. Biochem.* **2018**, *555*, 50-54.
3. Sun, S.-K.; Wang, B.-B.; Yan, X.-P., A label-free near-infrared fluorescent assay for the determination of deoxyribonuclease I activity based on malachite green/G-quadruplexes. *Analyst* **2013**, *138*, 2592-2597.
4. Lee, C. Y.; Park, K. S.; Jung, Y. K.; Park, H. G., A label-free fluorescent assay for deoxyribonuclease I activity based on DNA-templated silver nanocluster/graphene oxide nanocomposite. *Biosens. Bioelectron.* **2017**, *93*, 293-297.
5. Li, H.; Wang, L.; Zhai, J.; Luo, Y.; Zhang, Y.; Tian, J.; Sun, X., Tetracyanoquinodimethane nanoparticles as an effective sensing platform for fluorescent nucleic acid detection. *Anal. Methods* **2011**, *3*, 1051-1055.
6. Zhang, L.; Guo, S.; Dong, S.; Wang, E., Pd nanowires as new biosensing materials for magnified fluorescent detection of nucleic acid. *Anal. Chem.* **2012**, *84*, 3568-3573.
7. Zhu, S.; Liu, Z.; Zhang, W.; Han, S.; Hu, L.; Xu, G., Nucleic acid detection using single-walled carbon nanohorns as a fluorescent sensing platform. *Chem. Commun.* **2011**, *47*, 6099-6101.
8. Tan, H.; Tang, G.; Wang, Z.; Li, Q.; Gao, J.; Wu, S., Magnetic porous carbon nanocomposites derived from metal-organic frameworks as a sensing platform for DNA fluorescent detection. *Anal. Chim. Acta* **2016**, *940*, 136-142.
9. Yang, S.; Liu, M.; Deng, F.; Mao, L.; Yuan, Y.; Huang, H.; Chen, J.; Liu, L.; Zhang, X.; Wei, Y., Biomimetic modification of silica nanoparticles for highly sensitive and ultrafast detection of DNA and Ag⁺ ions. *Appl. Surf. Sci.* **2020**, *510*, 145421.
10. Qi, X.; Hu, H.; Liang, L.; Lin, Y.; Liu, Y.; Sun, H.; Piao, Y., Fluorescence nanoprobes bearing low temperature-derived biochar nanoparticles as efficient quenchers for the detection of single-stranded DNA and 17β-estradiol and their analytical potential. *RSC Adv.* **2024**, *14*, 28077-28085.

11. Wang, H.; Song, S.; Hao, J.; Song, A., Hydrogels triggered by metal ions as precursors of network CuS for DNA detection. *Chem. - Eur. J.* **2015**, *21*, 12194-12201.